ICARUS 112, 27–33 (1994)

A 360-Degree and -Order Model of Venus Topography

NICOLE RAPPAPORT AND JEFFREY J. PLAUT

Jet Propulsion Laboratory, California Institute of Technology, 4800 Oak Grove Drive, Pasadena, California 91109
E-mail: njb@nomad.jpl.nasa.gov

Received June 1, 1994; revised September 9, 1994

This report presents the most recent spherical harmonic topography model of Venus developed at Jet Propulsion Laboratory. It was produced by a spherical harmonic analysis of the most complete set of Magellan altimetry data, augmented by Pioneer Venus and Venera data. The harmonic coefficients of the topography were computed to degree and order 360. Compared to previous topography models, this one has the highest correlation with the gravity field of Venus. © 1994 Academic Press, Inc.

I. INTRODUCTION

This report provides the scientific community with the latest spherical harmonic topographic model of Venus produced at the Jet Propulsion Laboratory (JPL). The data set that was used is described in Section II. Section III presents the harmonic analysis of Venus' topography. Section IV presents scientific implications. Section V contains a summary.

II. DATA

The starting point for building the set of data that were analyzed was the GTDR files, which contain maps of Magellan altimetry data, produced by the Massachusetts Institute of Technology for the Magellan Project (Ford and Pettengill 1992). These data cover the planet by means of three maps: a Mercator projection map and two polar maps. These maps provide the most internally consistent version of the Magellan altimetry data set (P. Ford, personal communication). The maps were projected and averaged into a cylindrical grid of 0.25° x 0.25°. The original data have a pixel size of ≈5 km. Hence, the reprojection process reduces the resolution of the data set, especially at low latitudes. Overall, every sample of our topography model is based on a number of Magellan altimetry data points.

We follow Bills and Kobrick (1985) and Konopliv *et al.* (1993) and use a rectangular grid. This is intuitively justified from the behavior of the harmonic functions: each harmonic function has the same number of zeroes on each parallel. Furthermore, because of the method that we use to compute the harmonic coefficients, each data point is effectively weighted by the area of the corresponding cell.

The pre-Magellan topography model (TOPODR.4.0; Yewell 1993), which consisted of data from Pioneer Venus Orbiter (PVO) altimetry merged with Venera 15/16 altimetry, was used to fill gaps.

At this point, three gaps remained in the data. The two main gaps are located near the south pole, and a smaller gap is present near the north pole. These gaps have two separate origins: orbits during superior conjunction and orbits affected by the thermal hide strategy, in which the High Gain Antenna was used to shadow the spacecraft, precluding altimetry observations.

Our first topography model of Venus used a less complete set of Magellan and PVO altimetry data and a least squares method to compute the harmonic coefficients of the topography to order and degree 21 (McNamee *et al.* 1993). The least squares method did not require that the gaps be filled. Our second topography model used a more complete set of data and a computation by quadrature to obtain the coefficients to degree and order 120 (Konopliv *et al.* 1993). This new method required that no gap be present in the data. Therefore, we filled the gaps by using topographical heights computed from the 21 x 21 model. The same quadrature method is used in this paper. The gaps were filled by using the 120 x 120 model. Finally, we obtained a complete set of data referenced to the Venus body-fixed reference frame, as defined by Davies *et al.* (1992).

III. HARMONIC ANALYSIS OF THE TOPOGRAPHY

The planetary radius at latitude φ and longitude λ with respect to the body-fixed reference frame defined by the Venus rotation axis and prime meridian is written as

0019-1035/94 $6.00

$$= R_t \sum_{\ell=0}^{+\infty} \sum_{m=0}^{\ell} P_{\ell m}(\sin\varphi) \quad (C'_{\ell m}\cos m\lambda + S'_{\ell m}\sin m\lambda), \tag{1}$$

, is the equatorial radius, the $C'_{\ell m}$ and $S'_{\ell m}$ are the ·ed harmonic coefficients of the topography and arc the normalized Legendre functions.

Method

arc Iwo methods of computing the harmonic coef- of the topography. The first method consists of east squares fit of Eq. (1) to the data. In practice, squares method requires too much computing en the desired degree is high, A much less compu- y expensive method consists of computing the c coefficients independently, as integrals. The c coefficients arc given by

$$C'_{\ell m} = \frac{1}{4\pi R_0}\int_{-\pi/2}^{\pi/2} \cos\varphi\, d\varphi \int_0^{2\pi} d\lambda (R(\varphi, \lambda) - R_0) P_{\ell m}(\sin\varphi)\cos m\lambda,$$

$$S'_{\ell m} = \frac{1}{4\pi R_0}\int_{-\pi/2}^{\pi/2} \cos\varphi\, d\varphi \int_0^{2\pi} d\lambda (R(\varphi, \lambda) - R_0) P_{\ell m}(\sin\varphi)\sin m\lambda, \tag{2}$$

$_0$ is an a priori reference radius. These coefficients ive to R_0. They arc resealed by introducing a new e radius R_t such that $C_{00} = 1$.

ctice, the integral over the unit sphere must be by a sum of terms. Each term corresponds to l—defined by $\varphi_i - \delta\varphi/2 \le \varphi \le \varphi_i + \delta\varphi/2$, $\lambda_j - \ldots \le \lambda_j + \delta\lambda/2$ with $\delta\varphi = \delta\lambda = 0.25°$. Furthermore, ıust be modified to take into account the fact that e of the planetary radius in each pixel is a mean er that pixel. Wc used the procedure devised by (1993) to compute the integrals.

Results

ırmonic coefficients of the topography were com- individual integrals to degree and order 360. The dius of Venus is found to be R_t = 6051,848 km. determinations led to R_t = 6051.448 km (Bills ›rick 1985), R_t = 6051,839 km (McNamee *et al.* ıd R_t = 6051.839 km (Konopliv *et* al. 1993), The e between Bills and Kobrick determination and ruminations by McNamee *et al.* and Konopliv et e to the fact that Bills and Kobrick used prelimi- 0 data that were not completely reduced (Ford he difference between the two latter determina- d ours is due to the fact that the altimetry data that wc used in this paper were substantially improved with respect to the data used in the two previous papers. This improvement is a consequence of a reduction in the orbital errors.

TABLE I
Normalized Harmonic Coefficients of the Topography to Degree 5

ℓ	m	$C_{\ell m}$	$S_{\ell m}$
1	0	(- 1.0579 ± 0.02) x 10^{-6}	
1	1	(- 1.94395 0.001) X 10^{-5}	(1 .7864 ± 0.003) × 10^{-5}
2	0	(- 2.5917 ± 0.002) x 10^{-5}	
2	1	(1 .4489 ± 0.002) x 10"5	(- 8.S4S6 ± 0.03) x 10^{-6}
2	2	(- 2.1616 ± 0.002) x 10 '5	(- 3.3037 ± 0.01) X 10^{-6}
3	0	(3,0047 ± 0.002) x 10"5	
3	1	(4.7410 ± 0.002) X 10^{-5}	(- 7.9826 ± 0.02) x 10^{-6}
3	2	(4.4193 ± 0.03) x 10^{-6}	(2.3180 ± 0.004) × 10^{-5}
3	3	(- 9.1018 ± 0.02) X 10-'	(- 8.0818 ± 0.02) X 10^{-6}
4	0	(2.6756 ± 0.0006) x 10^{-5}	
4	1	(6.8970 ± 0.03) x 10^{-6}	(1.4741 ± 0.006) × 10^{-5}
4	2	(1.5841 ± 0.002) x 10^{-5}	(8.3783 ± 0.03) × 10^{-6}
4	3	(- 4.71425 0.02) x 10^{-6}	(- 3,7S23 ± 0.01) x 10^{-5}
4	4	(8.4789 ± 0.03) X 10-6	(3,0146 ± 0.003) × 10^{-5}
5	0	(- 8.7303< 0.02) x 10^{-6}	
5	1	(2.0695 ± 0.002) x 105	(2.3163 ± 0.001) × 10^{-5}
5	2	(4.0665 ± 0.02) x 10^{-6}	(- 1.3484 ± 0.003) X 10^{-5}
5	3	(7,6344 ± 0.03) x 10^{-6}	(1.88s0 ± 0.001) x 10^{-5}
5	4	(8,6339 ± 0.02) x 10^{-6}	(6,4104 ± 0.2) x 10^{-7}
5	5	(1,0987 ± 0.0008) x 10-s	(-7,8237 ± 0.01) x 10^{-6}

The harmonic coefficients up to degree 2 arc given in Table 1, In order to obtain an order of magnitude of the uncertainties in the coefficients, wc performed three additional calculations in which the data where modified by adding ± 80 m to each data point, where the sign was chosen randomly for each point. The uncertainties listed in Table 1 correspond to the maximum difference between the nominal case and the three cases where the data quality had been artificially degraded. These uncertainties are pessimistic, first because the error of ± 80 m is itself pessimistic, and then because they cumulate the errors made in the three cases where the data were degraded, On the other hand, the method that wc used to evaluate the uncertainties in the individual coefficients assumes that the errors in the topographic heights are uncorrelated and dots not take into account the over-sampling near the pole, and in that sense it may be optimistic.

Figure 1 shows topography contours obtained with our topography model. Figure 2, which shows the topography along the equator, both as given by the data (continuous line) and as computed from the model (black triangles), indicates that there is a good agreement between the model and the data. Figure 3 contains a plot of the difference between the topography along the equator computed from the model and the observed topography. This plot

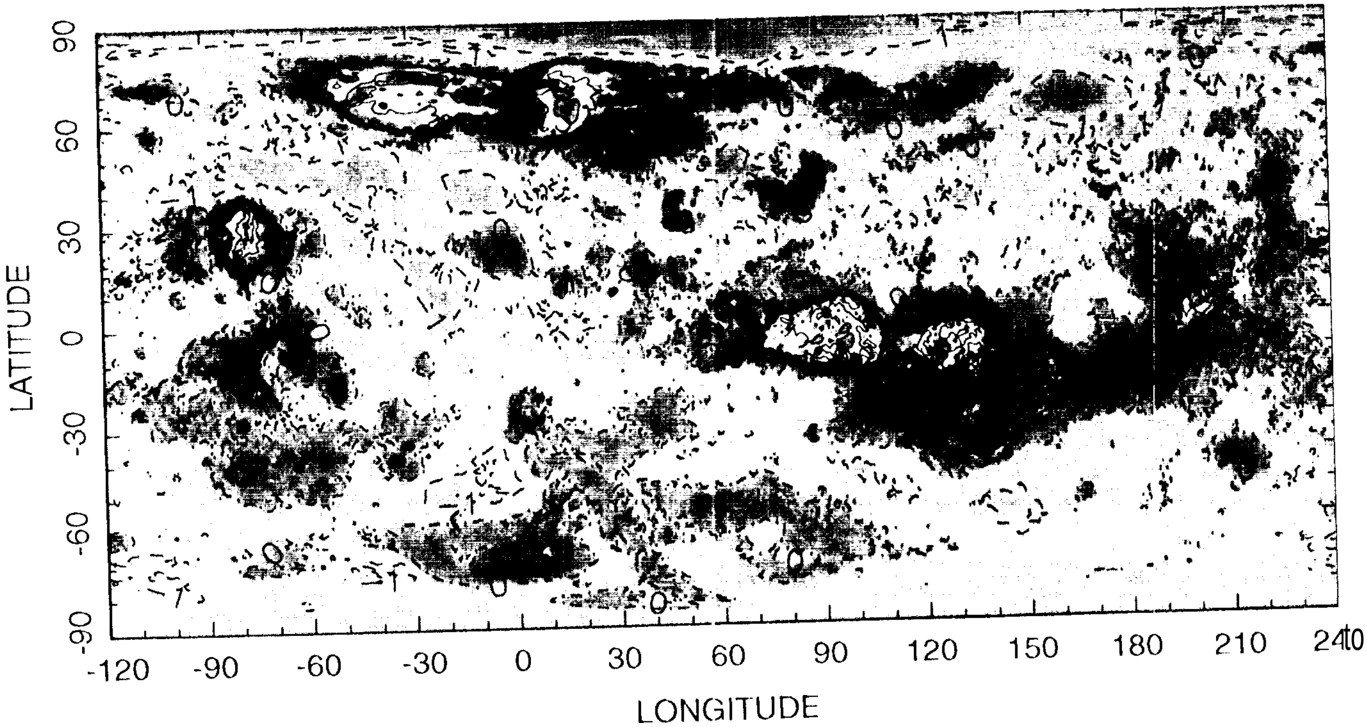

FIG. 1. Topography map produced by using this paper's 360× 360 topography model. The zero level correspond to Venus' mean radius R_r = 6051.848 km. The topography contours are separated by 1 km.

shows that the error in the model is due to the high-frequency terms.

Our topography model can be obtained by writing to the authors of the paper and it will be archived in the Planetary Data System Geosciences Node at Washington University (Saint Louis, MO).

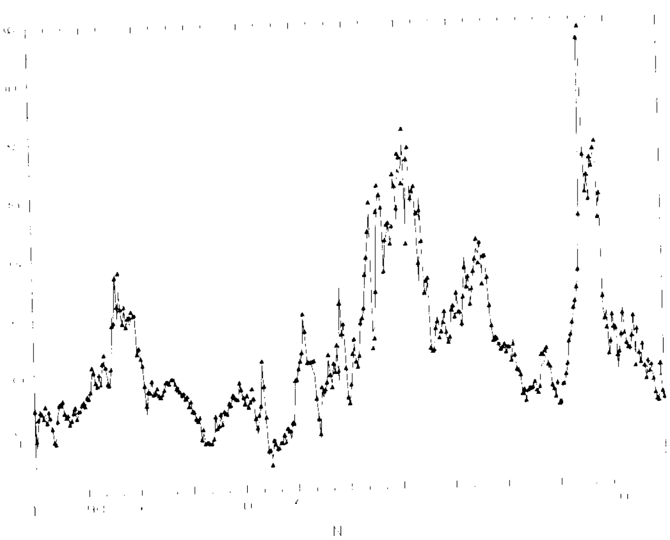

FIG. 2. Topography along the equator from the data (continuous line) and as computed from our model (black triangles), with respect to the reference radius. The vertical scale is in kilometers.

IV. IMPLICATIONS

This section is devoted to scientific results obtained from our model.

IV.1, Geometrical Implications

Since the flattening of Venus is very small, its topography can be approximated by a sphere offset from the origin of the coordinate system, which is Venus' center of mass. According to this definition of the offset between the center of mass and the center of figure, the location of the center of figure is given by

$$
\begin{aligned}
X_f &= R_r C_{11} = 118 \text{ m},\\
Y_f &= R_r S_{11} = 108 \text{ m},\\
Z_f &= R_r C_{10} = 6 \text{ m}.
\end{aligned}
\tag{3}
$$

The above definition is used by scientists who are interested in understanding the internal structure of Venus. On the other hand, there exist other areas of planetary sciences where scientists use approximations of planetary

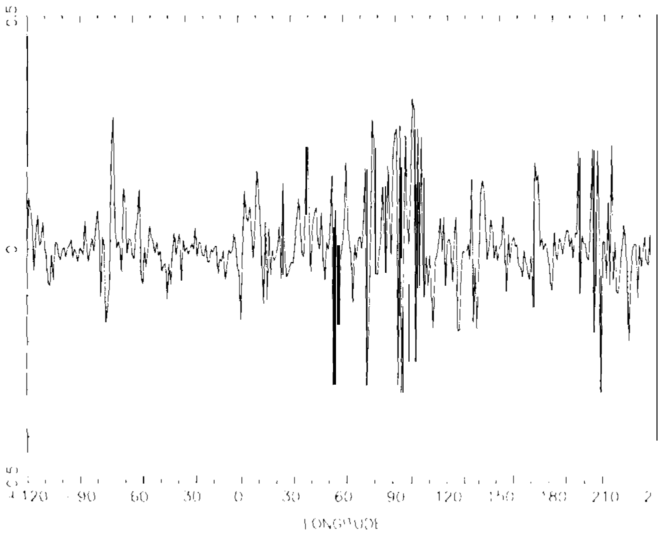

FIG. 3. Difference between the topography along the equator computed from the model and the observed topography. The vertical scale is in kilometers.

body's shapes as ellipsoids offset from the center of mass (Davies *et al.* 1992). An example of a situation in which the ellipsoid model is useful is that of occultation experiments.

To first order with respect to the harmonic coefficients, the location of the center of figure of the ellipsoid is given by Eq. (3). A more accurate method consists of fitting an offset ellipsoid by least squares to the topography. This calculation yields

$$X_f = -205 \text{ m},$$
$$Y_f = 181 \text{ m},$$
$$Z_f = 71 \text{ m},$$

which corresponds to the latitudinal coordinates

$$r_f = 282 \text{ m},$$
$$\varphi_f = 14°,$$
$$\lambda_f = 139°$$

and indicates that the center of figure lies under the northeast part of Thetis Regio.

The least square fit also gives the orientation and the length of the principal axes of figures. These are given in Table II, together with the orientation of the principal axes of inertia. The axes of figures and the axes of inertia do not coincide. The orientation of the axes of figures is governed by the equatorial and mid-latitude highlands. The longest axis of figure passes through Phoebe Regio and Niobe Planitia, North of Ovda in Western Aphrodite. The second axis of figure passes through Eistla Regio and South of Atla in Eastern Aphrodite.

IV.2. *Statistical Implications*

The rms magnitude of the normalized coefficient, defined by

$$\text{rms}(\ell) = \sqrt{\frac{\sum (C_{\ell m})^2 + (S_{\ell m})^2}{2\ell + 1}}, \tag{4}$$

where the sum goes from $m = 0$ to $m = \ell$ is shown on Fig. 4, in logarithmic scale. As in Section III.2, we degraded the topography data by adding randomly ±80 m to each data point in order to estimate uncertainties in the spectrum. Even though the individual coefficients change, the spectrum remains very stable and the curve corresponding to the degraded topography data practically coincide with the nominal curve.

For $\ell \gtrsim 100$, the slope of the spectrum changes and the spectrum becomes flatter. This may not be a real property of the spectrum but rather an artifact associated with our method. As mentioned in Section III.2, the errors in the topography model are essentially in the high-frequency terms. One possibility is that the oversampling at high latitude had the effect of producing too much power in the high-degree harmonic coefficients.

We compared the variance of the observed topography with the variance of the topography computed from our model. Denoting by f the topography, the variance was computed using the equation

$$\sigma_f = \frac{1}{S} \int_{-\pi/2}^{\pi/2} \int_0^{2\pi} [f(\varphi, \lambda) - \bar{f}]^2 \, dS, \tag{5}$$

where dS represents an element of surface and

TABLE II

Orientation of the Principal Axes of Figures and of the Principal Axes of Inertia of Venus

	Axes of figure	Axes of inertia
Latitude	13.8°	0.2°
Longitude	98.2°	-2.9°
Length	6052.3 km	
Latitude	23.3°	0.4°
Longitude	11.2°	87.1°
Length	6051.8 km	
Latitude	64.9°	89.5°
Longitude	168.4°	117.3°
Length	6051.4 km	

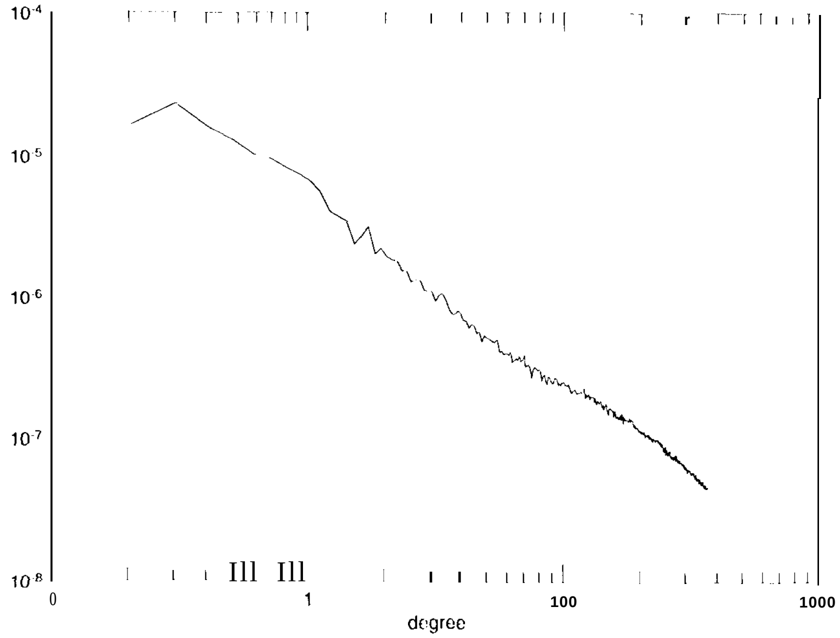

FIG. 4. Rms magnitude of the normalized coefficient of the topography on a logarithmic scale.

$$\bar{f} = \frac{1}{S}\int_{-\pi/2}^{\pi/2}\int_0^{2\pi} f(\varphi, \lambda)\, dS. \quad (6)$$

With the observed topography, we obtained $\sqrt{\sigma_f} =$ 0.943 while our model gives an almost equal value of $\sqrt{\sigma_f} =$ 0,941. The agreement between these two values is due to the fact that the variance is essentially due to the low-degree terms and does not allow one to rule out that the model overestimates the power of the high-degree harmonic coefficients.

The correlation between Venus' topography and gravity was also investigated. The gravity field at a point P outside the planet is

$$U(r, \varphi, \lambda) = \frac{GM}{r}\sum_{\ell=2}^{+\infty}\sum_{m=0}^{\ell}\left(\frac{R_g}{r}\right)^{\ell} P_{\ell m}(\sin\varphi)(C^g_{\ell m}\cos m\lambda + S^g_{\ell m}\sin m\lambda), \quad (7)$$

where G is the gravitational constant, M is the mass of the planet, R_g is a reference radius, and the $C^g_{\ell m}, S^g_{\ell m}$ are the harmonic coefficients of the gravity field.

The correlation per degree was computed as

$$\gamma(\ell) = \frac{\sum C^t_{\ell m}C^g_{\ell m} + S^t_{\ell m}S^g_{\ell m}}{\sqrt{\sum (C^t_{\ell m})^2 + (S^t_{\ell m})^2}\sqrt{\sum (C^g_{\ell m})^2 + (S^g_{\ell m})^2}}, \quad (8)$$

where the sums go from $m = 0$ to $m = \ell$. It is shown in Fig. 5 for three topography models, the one by Konopliv *et al.* (1993), the one by Balmino (1993), and the model presented in this paper. All calculations used the most recent gravity field model of Konopliv and Sjogren (1994). The uncertainty in the correlation due to the errors in the harmonic coefficients of the topography was computed

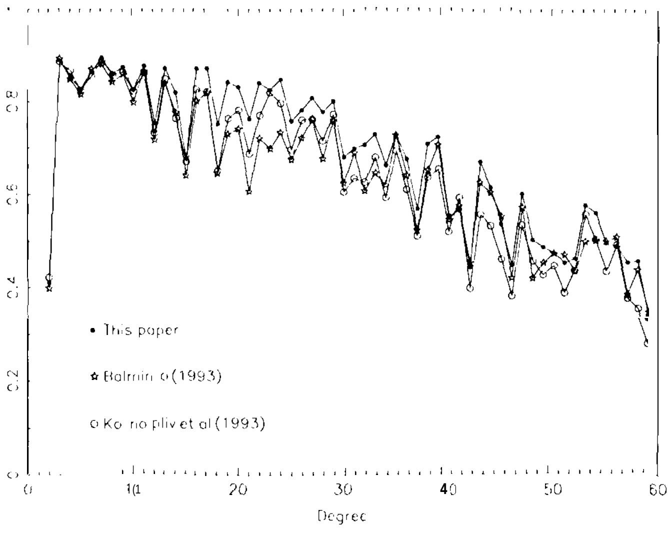

FIG. 5. Correlation per degree between Venus' topography and its gravity field, comparing the topography model of Konopliv *et al.* (1993), the model of Balmino (1993), and this paper's topography model; all calculations use the most recent gravity field model of Konopliv and Sjogren (1994).

TABLE III
Correlations between Venus' Topography and Its Gravity Field over Seven Regions and over the Entire Planet

Regio	φ_{min}	φ_{max}	λ_{min}	λ_{max}	γ_1	γ_2	γ_3
Beta	10°	40°	105°	55°	0.877	0.819	0.934
Phoebe	25°	10°	-90°	50°	0.765	0.821	0.845
Maxwell	45°	80°	60°	30°	0.842	0.857	0.864
Gula	0°	30°	15°	30°	0.890	0.897	0.918
Bell	0°	40°	30°	60°	0.77[illegible]	0.799	0.812
Ovda	15°	10°	75°	110°	0.790	0.794	0.805
Atla	10°	30°	180°	210°	0.949	0.964	0.968
Planet	90°	90°	120°	240°	0.753	0.745	0.772

Note. γ_1 is based on the topography model of Konopliv *et al.* (1993); γ_2 uses the topography model of Balmino (1993); γ_3 is based on this paper's topography model; all calculations use the most recent gravity field model of Konopliv and Sjogren (1994).

as above. by comparing the nominal correlation with the correlation obtained by degrading the topography data. We found that it was negligible. The error bars due to the errors in the gravity field coefficient are shown in Fig. 10 of Konopliv and Sjogren (1994).

Balmino's model was obtained from a least squares procedure. Balmino (1993) checked that the two methods give the same results if the same data sets are used.

Our model has the highest correlation with the gravity field. Since it is very unlikely that this highest correlation is due to chance, we infer that the highest correlation indicates improvement over previous models.

The correlation at degree 2 is much less than for the other low-degree harmonic coefficients. This is probably related to the fact that Venus' rotation has been tidally slowed down over the age of the Solar System and the harmonic coefficients of degree 2 have nothing to do with adjustment to hydrostatic equilibrium.

We also computed regional correlations in the following way. Denoting by g the gravity at the surface and using Eqs. (6) and (5) to compute $\bar{g}$ and σ_g, the regional correlation is given by

$$\gamma = \frac{(1/S) \int\int (f - \bar{f})(g - \bar{g}) \, dS}{\sqrt{\sigma_f \sigma_g}}. \qquad (9)$$

Regional correlations over seven regions of Venus are listed in Table III for the three above-mentioned topography models. Again, our model gives the highest correlations. Among the seven regions that we studied, the highest correlations are obtained in Beta Regio and Atla Regio. These highlands are also characterized by moderately negative Bouguer anomalies and abundant volcanism which suggest dynamic support of the topography. The lowest correlations were obtained in Ovda Regio. Ovda is characterized by very large negative Bouguer anomalies and complex ridged terrains or tesserae, which suggest essentially passive isostasy associated with crustal thickening.

V. SUMMARY

The first purpose of this paper is to make available to the scientific community the best model developed at the JPL. Models of Venus topography in spherical harmonics are useful for studying the geophysics of this planet. Examples of recent work using such models are found in Banerdt *et al.* (1994), Kucinskas and Turcotte (1994), and Simmons *et al.* (1994).

The second purpose of this paper is to present some geometrical and statistical implications of this model. The scientific conclusions are:

(a) The offset between the center of mass and the center of figure is about 10 times smaller than the offset in Earth, the Moon, and Mars. The center of figure of Venus lies under Aphrodite.

(b) The orientation of the principal axes is determined by the equatorial and mid-latitude highlands.

(c) The topography and the gravity field of Venus are very strongly correlated. Regional correlations are higher in Beta Regio and Atla Regio, which are thought to be dynamically supported, than in Ovda Regio, which is thought to be essentially supported by passive isostasy.

(d) The rms spectrum of the topography follows a power law up to degree $\ell \sim 100$. The flattening of the rms spectrum for $\ell > 100$ may not be real.

REFERENCES

BALMINO, G. 1993. The spectra of the topography of the Earth, Venus and Mars. *Geophys. Res. Lett.* 20, 1063–1066.

BANERDT, W. B., A. S. KONOPLIV, N. J. RAPPAPORT, W. L. SJOGREN, R. E. GRIM, AND P. G. FORD 1994. The isostatic state of Mead Crater, *Icarus* 112, 117–129.

BILLS, B. G., AND K. KOBRICK 1985. Venus topography: A harmonic analysis. *J. Geophys. Res.* 90, 827–836.

DAVIES, M. E., V. K. ABALAKIN, M. BURSA, T. LEDERLE, J. H. LIESKE, R. H. RAPP, P. K. SEIDELMAN, A. T. SINCLAIR, V. G. TEJFEL, AND V. S. TJUFLIN 1992. Report of the IAU/IAG/COSPAR Working group on cartographic coordinates and rotational elements of the planets and satellites: 1991. *Celest. Mech.* 53, 377–397.

FORD, G. 1986. *Pioneer Venus hypsometry*. MIT memorandum, Massachusetts Institute of Technology, Cambridge.

FORD, P. G., AND G. H. PETTENGILL 1992. Venus topography and kilometer-scale slopes, *J. Geophys. Res.* 97, 13,103–13,114.

KONOPLIV, A. S., N. J. BORDERIES, P. W. CHODAS, E. J. CHRISTENSEN, W. L. SJOGREN, B. G. WILLIAMS, G. BALMINO, AND J. P. BARRIOT 1993. Venus gravity and topography: 60th degree and order model. *Geophys. Res. Lett.* 20, 2403–2406.

KONOPLIV, A. S., AND W. L. SJOGREN 1994. Venus spherical harmonic gravity model 10 degree and order 60. *Icarus* 112, 42-54.

KUCINSKAS, A. B., AND D. L. TURCOTTE 1994. Isostatic compensation of equatorial highlands on Venus. *Icarus* 112, 104--116.

MCNAMEE, J. B., N. J. BORDERIES, AND W. L. SJOGREN 1993. Venus: Global gravity and topography. *J. Geophys. Res.* 98, 9113-9128.

SIMMONS, M., B. H. HAGER, AND S. C. SOLOMON 1994. Global variations in the geoid topography admittance of Venus. *Science* 264, 798-803.

YEWELL, S, U, 1993. *Magellan Data Product Information Handbook*. Magellan Document 630-512.